Tumstatin, a Matrikine Derived from Collagen Type IV3, is Elevated in Serum from Patients with Non-Small Cell Lung Cancer

Nielsen, Signe Holm; Willumsen, Nicholas; Pedersen, Susanne Brix; Sun, Shu; Manon-Jensen, Tina; Karsdal, Morten; Genovese, Federica

Published in:
Translational Oncology

Link to article, DOI:
10.1016/j.tranon.2018.02.005

Publication date:
2018

Document Version
Publisher's PDF, also known as Version of record

Translational Oncology
www.transonc.com

Volume 11 Number 2 April 2018 pp. 528–534 528

Tumstatin, a Matrikine Derived from Collagen Type IVα3, is Elevated in Serum from Patients with Non–Small Cell Lung Cancer

Signe Holm Nielsen*,†, Nicholas Willumsen*, Susanne Brix†, Shu Sun*, Tina Manon-Jensen*, Morten Karsdal* and Federica Genovese*

*Fibrosis Biology and Biomarkers, Nordic Bioscience A/S, Herlev, Denmark; †Disease Systems Immunology, Department of Biotechnology and Biomedicine, Technical University of Denmark, Lyngby, Denmark

Abstract

OBJECTIVES: Fibrosis and cancer are characterized by extracellular matrix (ECM) remodeling. The basement membrane is mainly composed by collagen type IV and laminin. Tumstatin is a matrix metalloproteinase-9 (MMP-9) generated matrikine of collagen type IV α3 chain. We evaluated the potential of tumstatin as a diagnostic biomarker of lung disorders. *METHODS:* A monoclonal antibody was raised against the neo-epitope tumstatin. A novel competitive enzyme-linked immunosorbent assay for detection of tumstatin (TUM), was developed and technically characterized. Levels of TUM were measured in serum of patients with idiopathic pulmonary fibrosis (IPF), chronic obstructive pulmonary disease (COPD), and non–small cell lung cancer (NSCLC) belonging to two cohorts. *RESULTS:* The developed TUM enzyme-linked immunosorbent assay (ELISA) was technically robust. In cohort 1, levels of TUM were significantly higher in NSCLC compared to healthy controls, IPF, and COPD ($P = 0.007$, $P = 0.03$ and $P = 0.001$, respectively). The area under the receiver operating characteristics (AUROC) for separation of patients with NSCLC from healthy controls was 0.97, for separation of NSCLC and IPF patients was 0.98, and for separation of NSCLC and COPD patients was 1.0. In cohort 2, levels of TUM were also significantly higher in patients with NSCLC compared to healthy controls ($P = 0.002$), and the AUROC for separation of NSCLC and healthy controls was 0.73. *CONCLUSIONS:* We developed a technically robust competitive ELISA targeting the fragment tumstatin. The level of TUM in circulation was significantly higher in patients with NSCLC compared to patients with IPF, COPD and healthy controls. The assay provided high diagnostic accuracy in separating NSCLC patients from other lung disorders and from healthy controls.

Translational Oncology (2018) 11, 528–534

Introduction

The extracellular cellular matrix (ECM) is the noncellular component of all organs and tissues. Altered ECM remodeling plays a vital role in diseases such as fibrosis and cancer [1]. The basement membrane (BM) is a specialized ECM which functions as a scaffold for epithelial and endothelial cells, acts as a barrier between tissues, and supports tissue structure by maintaining epithelial and endothelial cell polarity and function [2,3]. The BM also serves as a barrier for cancer cell invasion. Breaching of the BM and loss of BM integrity are associated with an invasive cancer phenotype [4]. The BM is also remodeled as part of angiogenesis. During angiogenesis, the endothelial cells are induced to proliferate and migrate by signaling molecules generated by the degradation of the adjacent BM by proteolytic enzymes. BM degradation leads in fact to exposure of protein domains (so called "cryptic sites") or protein fragments with either proangiogenic or antiangiogenic activity. One of the best-described fragments is the matrikine endostatin, a known inhibitor of angiogenesis and tumor growth [5].

The two main BM proteins are collagen type IV and laminin, which together form a distinct network linked together by nidogen and heparin sulfates [3,6–8]. Collagen type IV is formed by the

Address all correspondence to: Signe Holm Nielsen, Nordic Bioscience, Herlev Hovedgade 205-207, 2730 Herlev. E-mail: shn@nordicbio.com
Received 10 January 2018; Revised 12 February 2018; Accepted 14 February 2018

1936-5233/18
https://doi.org/10.1016/j.tranon.2018.02.005

combination in heterotrimers of six different α-chains (α1-6) in the mammalian BMs [9]. The α3 chain of collagen type IV (COL4α3) has been described to have restricted distribution across BMs and is primarily found in the lungs and kidneys [10]. The structural role of COL4α3 is illustrated by clinical manifestations of Alport's syndrome, Goodpasture's syndrome, idiopathic pulmonary fibrosis (IPF), and lung cancer, which are characterized by damage to COL4α3 by either mutations, immune attacks or leaky vasculature and altered BM composition [11–14].

Tumstatin is a 28-kDa fragment of COL4α3 that binds to endothelial cells via the αvβ3 integrin [15]. It is a matrikine generated by matrix metalloproteinase-9 (MMP-9) and known to keep pathological angiogenesis and tumor growth in check [15–17]. MMP-9 is needed to cleave tumstatin from COL4α3 and function as a protective matrikine. Lack of MMP-9 accelerates tumor growth in MMP-9 knockout mice, while high COL4α3 expression correlates with poor prognosis in patients with lung cancer [17,18]. This collagen chain therefore has both protective and tumor-promoting capabilities.

Several studies have hypothesized the potential of matrikines, such as tumstatin, as biomarkers of pathology; however, no such marker is currently available [13,19–21].

Our hypothesis was that tumstatin is a potential biomarker for lung disorders reflecting degradation of the BM. We therefore developed and validated a novel neo-epitope specific competitive enzyme-linked immunosorbent assay (ELISA) targeting tumstatin (TUM), and measured the concentration of TUM in serum samples of patients diagnosed with different lung disorders, including IPF, chronic obstructive pulmonary disease (COPD), and non–small cell lung cancer (NSCLC) and investigated its potential as a diagnostic biomarker.

Materials and Methods

All reagents used for the experiments were high-quality standards from Sigma Aldrich (St. Louis, MO) and Merck (Whitehouse Station, NJ). The synthetic peptides used for immunization and assay development were purchased from American Peptide Company (Sunnyvale, CA).

Generation of Monoclonal Antibodies

The amino acid sequence ^{1426}'PGLKGKRGDS'^{1436} in the human α3 chain of type IV collagen was used for the generation of monoclonal antibodies (mAbs). The corresponding sequence in rat has one mismatch in position 6, and in mouse, it has a mismatch in position 5 (Figure 1). Immunization was initiated by subcutaneous injection of 200 μl emulsified antigen and 100 μg immunogenic peptide (PGLKGKRGDS–GGC-KLH) in 4- to 6-week-old Balb/C mice using Stimmune (Thermo Fisher). The immunizations were repeated every second week until stable serum antibody titer levels were reached. The mouse with the highest serum titer was selected for fusion and rested for a month. Subsequently, the mouse was boosted intravenously with 50 μg immunogenic peptide in 100 μl 0.9% NaCl solution 3 days before isolation of the spleen for cell fusion. To produce hybridoma cells, the mouse spleen cells were fused with SP2/0 myeloma cells as described by Gefter et al. [22]. Subsequently, the clones were plated into 96-well microtiter plates for further growth, and the limiting dilution method was applied to promote monoclonal growth. An indirect ELISA performed on streptavidin-coated plates was used for the screening of supernatant reactivity. PGLKGKRGDS-K-Biotin was used as screening peptide, while the standard peptide PGLKGKRGDS was used to further test the specificity of the clones. Supernatant was collected from the hybridoma cells and purified using HiTrap affinity columns (GE Healthcare Life Science, Little Chalfront, Buckinghamshire, UK) according to manufacturer's instructions.

Clone Characterization

Native reactivity was assessed using human serum and human urine purchased from a commercial supplier (Valley Biomedical, Winchester, VA). The cleavage site is localized at the N-terminal of the sequence; therefore, the mAb was selected to specifically recognize the standard peptide starting at the cleavage site (PGLKGKRGDS) and not a sequence elongated or truncated of one amino acid (IPGLKGKRGDS and GLKGKRGDS, respectively). The isotype of the monoclonal antibody was determined using the Clonotyping System-HRP kit, cat. 5300-05 (Southern Biotech, Birmingham, AL).

TUM ELISA

The TUM competitive ELISA procedure was as follows: 96-well streptavidin-coated ELISA plates (Roche, cat. 11940279) were coated with 10 ng/ml biotinylated peptide PGLKGKRGDS-K-Biotin dissolved in assay buffer (25 mM Tris-BTB 2g. NaCl/L, pH 8.0), 100 μl/well, and incubated for 30 minutes at 20°C in the dark with 300 rpm shaking. Plates were washed five times in washing buffer (20 mM TRIS, 50 mM NaCl, pH 7.2). Subsequently, 20 μl of standard peptide or sample was added to appropriate wells, followed by 100 μl of 7 ng/ml horseradish peroxidase–labeled monoclonal antibody solution. The plates were incubated for 1 hour at 20°C with 300 rpm shaking and subsequently washed in washing buffer. Finally, 100 μl 3,3',5,5-tetramethylbenzinidine (TMB) (Kem-En--Tec cat. 438OH) was added and incubated for 15 minutes at 20°C with 300 rpm shaking. To stop the enzyme reaction of TMB, 100 μl of stopping solution (1% H_2SO_4) was added. The plate was analyzed by an ELISA reader at 450 nm with 650 nm as reference (VersaMax; Molecular Devices, Sunnyvale, CA). A standard curve was performed by serial dilution of the standard peptide and plotted using a four-parametric mathematical fit model. Standard concentrations were 0, 0.3125, 0.625, 1.25, 2.5, 5, 10, and 20 ng/ml. Each plate included five kit controls to monitor intra- and interassay variation. All samples were measured within the range of the assay, and all samples below lower limit of measurement range (LLMR) were reported as the value of LLMR.

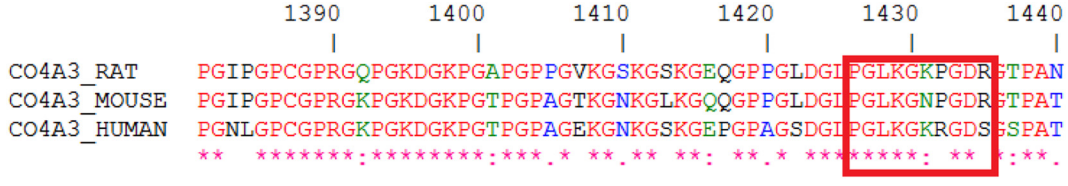

Figure 1. Sequence alignment between human, mouse, and rat tumstatin. The antibody recognizes residues from 1426 to 1436.

Technical Evaluation

Two-fold dilutions of four human serum and human urine samples were used to assess linearity. Linearity was calculated as a percentage of recovery of the undiluted sample.

Antibody specificity was calculated as percentage of signal inhibition by two-fold diluted standard peptide (PGLKGKRGDS), elongated peptide (LPGLKGKRGDS), truncated peptide (GLKGKRGDS), and non-sense peptide (LRSKSKKFRR). The intra- and interassay variation was determined by 10 independent runs of five quality controls and two kit controls run in double determinations. Accuracy of the assay was measured in healthy human serum/urine samples spiked with standard peptide and a serum/urine sample with a known high TUM concentration, and calculated as the percentage recovery of the measured value and the expected concentration of the peptide or the serum/urine sample with high TUM plus the concentration of the analyte in serum/urine. Interference was measured in healthy human serum spiked with biotin (low = 30 ng/ml, high = 90 ng/ml), hemoglobin (low = 0.155 mM, high = 0.310 mM), or lipids (low = 4.83 mM, high = 10.98 mM). The interference was calculated as the percentage recovery of the analyte in nonspiked serum. Furthermore, the interfering effect of human anti-mouse antibody (HAMA) was evaluated. Five healthy human serum samples were added to a panel of different HAMA concentration. These were analyzed with and without 5% Liquid II (Osteocalcin EIA Puf-Liq by Roche Diagnostics) in the dilution buffer, which counteracts the interference by HAMA. Salt interference was tested by measuring salt samples with a concentration of 8.14 g/l NaCl at pH 7.0 and 8.0. To define the concentration of TUM in the healthy population, 32 healthy human serum samples were measured, and the relation of the marker concentration to age and gender of the sample donors was evaluated. LLMR and upper limit of measurement range (ULMR) were calculated based on the 10 individual standard curves from the intra- and interassay variation. The analyte stability was determined for three healthy human serum samples incubated at either 4 or 20°C for 2, 4, and 24 hours. The stability of the samples was evaluated by calculating the percentage variation from the sample kept at 20°C (0 hour sample). Furthermore, the analyte stability was determined for three healthy human serum samples exposed to four freeze and thaw cycles. To assess the stability of the analyte, the percentage recovery of the analyte was calculated from the sample that underwent only one freeze/thaw cycle.

Biological Validation of TUM

TUM was measured in serum samples from two different cohorts. Both cohorts were obtained from the commercial vendor Proteogenex (Culver City, CA). Samples were collected after informed consent and approval by the local Ethics Committee and in compliance with the Helsinki Declaration of 1975.

Cohort 1 included patients diagnosed with IPF, COPD, NSCLC and colonoscopy-negative controls with no symptomatic or chronic disease. Patient demographics are shown in Table 2. Cohort 2 included patients diagnosed with NSCLC in cancer stage I, II, III, and IV together with colonoscopy-negative controls with no symptomatic or chronic disease. Patient demographics of this cohort can be found in Table 3.

Ethical Statement

The production of monoclonal antibodies performed in mice was approved by the National Authority (The Animal Experiments Inspectorate) under approval number 2013-15-2934-00956. All animals were treated according to the guidelines for animal welfare.

Statistical Analysis

Characteristics of the cohorts are presented as a number (frequency) and percentage for categorical variables and mean (standard deviation) for continuous variables. Statistical differences for categorical were assessed using a Kruskal-Wallis test (nonparametric) for cohort 1 and a Mann-Whitney *t* test in cohort 2. Results are shown as a Tukey boxplots. The diagnostic power of TUM was investigated by the area under the receiver operating characteristics (AUROC) curve. For all statistical analyses performed, a *P* value below .05 was considered significant. Asterisks indicate the following: $^{*}P < .05$; $^{**}P < 0.01$. Statistical analysis and graphs were performed using GraphPad Prism version 7 (GraphPad Software, Inc., La Jolla, CA).

Results

Clone Characterization

The best antibody producing hybridomas were screened for reactivity towards the standard peptide and native material in the competitive ELISA. Based on the reactivity, the clone NBH134#102-3GF was chosen for assay developed and determined to be the IgG1 subtype. Native reactivity was observed in human serum and urine (Figure 2), while no reactivity was found towards the elongated peptide, truncated peptide, non-sense standard peptide, and non-sense coater (Figure 3).

Technical Evaluation of the TUM ELISA Assay

A full technical validation was performed to evaluate the TUM ELISA assay. A summary of the validation data can be found in Table 1. The measurement range (LLMR-ULMR) of the assay was determined to be 0.26 to 9.92 ng/ml. The intra- and intervariation was 8.04% and 10.96%, respectively, based on 10 independent assays. Linearity of the human samples was observed from undiluted to four-fold dilution for human serum, and undiluted to two-fold dilution for human urine. Spiking recovery of standard peptide in human serum, and human serum in human serum resulted in a mean recovery of 90% and 99%, respectively. Hemoglobin, lipids, and biotin did not interfere with measurements of the TUM analyte in human serum. The stability of

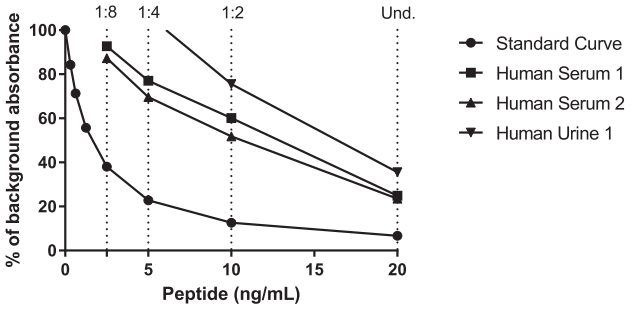

Figure 2. Assay linearity. Inhibition curves for the standard peptide and native material (human serum and human urine). The standard peptide was two-fold diluted starting from 20 ng/ml. The samples were tested undiluted and up to eight-fold diluted as indicated. The data are presented as percentage (%) of background absorbance, which is the absorbance of the assay buffer, as a function of peptide concentration.

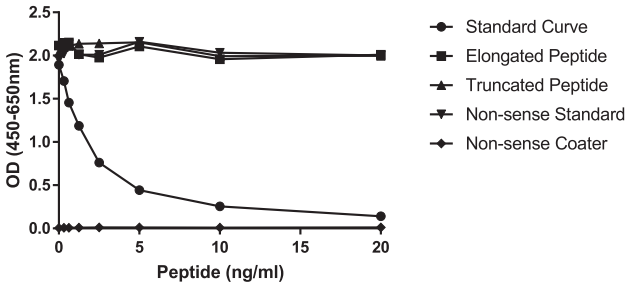

Figure 3. Assay specificity. Inhibition curves for to the standard peptide (PGLKGKRGDS), the elongated peptide (LPGLKGKRGDS), the truncated peptide (GLKGKRGDS), and a non-sense peptide (LRSKSKKFRR) in the TUM assay. The peptides were two-fold diluted starting from 20 ng/ml. The background signal was tested using a non-sense coating peptide (Biotin-LRSKSKKFRR). The data are presented as absorbance as a function of peptide concentration.

the analyte was acceptable during both prolonged storage of human serum samples at 4°C and 20°C (102.4% and 80.1%) and during freeze/thaw cycles (80.8%).

Biological Evaluation – TUM as a Biomarker for Lung Cancer

TUM was measured in serum of patients with lung disorders from two independent cohorts: cohort 1 and cohort 2.

Cohort 1 consists of healthy controls and patients diagnosed with IPF, COPD, and NSCLC. TUM was significantly elevated in serum from NSCLC compared to healthy controls, IPF patients, and COPD patients (P = 0.007, P = 0.03, and P = 0.001, respectively) (Figure 4). No significant difference was observed between healthy controls, IPF patients, and COPD patients, which indicated that TUM may play a role in NSCLC but not in fibrotic lung disorders.

In cohort 2, TUM was measured in samples from healthy controls and patients with NSCLC. TUM was significantly upregulated in patients with NSCLC compared to healthy controls (P = .002) (Figure 5). TUM was not significantly different between the different cancer stages.

The AUROC was used to evaluate the diagnostic power of TUM to separate NSCLC and healthy controls. As shown in Table 4, TUM was able to discriminate between NSCLC patients and healthy controls in cohort 1 with an AUROC of 0.97, NSCLC patients and IPF patients with an AUROC 0.98, and NSCLC and COPD patients with an AUROC of 1.00.

In cohort 2, TUM was able to discriminate between NSCLC patients and healthy controls with an AUROC 0.73. We furthermore saw that diagnostic accuracy increased with disease stage. These findings indicate that serological TUM levels could be used to separate healthy controls from patients with NSCLC with a high diagnostic accuracy.

Table 1. TUM ELISA Technical Validation Data

Technical Validation Test	Result
IC50	1.6 ng/ml
Detection range	0.26-9.92 ng/ml
Intraassay variation [a]	8.04%
Interassay variation [a]	10.96%
Dilution recovery of human serum [a]	89%
Dilution recovery of human urine [a]	98%
Analyte recovery 24 h, 4°C/20°C [a]	102.4%/80.1%
Hemoglobin recovery, low/high [a]	100%/100%
Lipemia recovery, low/high [a]	100%/100 %
Biotin recovery, low/high [a]	120%/106%
Salt recovery, pH 6.0/pH 7.0/pH 8.0 [b]	97 %
Spiking recovery (peptide in serum) [a]	90%
Spiking recovery (serum in serum) [a]	99%
Analyte recovery, 4 freeze/thaw cycles [a]	80.8%

[a] Percentages are reported as mean.
[b] Average recovery after salt interference.

Table 2. Patient Demographics of Cohort 1

	Healthy Controls (n = 8)	IPF (n = 7)	COPD (n = 8)	NSCLC (n = 8)	P-Value
Age	54.88 (7.85)	74.13 (8.36)	75.38 (1.69)	60.50 (9.32)	<0.001
Male, n (%)	6 (75%)	4 (57%)	4 (50%)	7 (87.5%)	0.102
BMI	26.25 (1.27)	25.79 (1.58)	27.24 (1.84)	N/A	0.170
FEV_1% of predicted value	-	64.38 (3.42)	61.50 (7.19)	-	0.634
FEV_1/FVC ratio %	-	76.00 (1.51)	58.38 (15.20)	-	0.016
TUM (ng/ml)	1.79	2.00	1.58	4.24	<0.001

Data are presented as mean (SD) unless otherwise stated. Comparison of age, gender, BMI, and TUM levels was performed using Kruskal-Wallis adjusted for Dunn's multiple comparisons test, while comparison of FEV_1% of predicted value and FEV_1/FVC ratio % was calculated using the Mann-Whitney unpaired t test. P values below .05 were considered significant. Abbreviations: *BMI*, body mass index; *FEV1*, forced expiratory volume in 1 second; *NSCLC*, non–small cell lung cancer; *FVC*, forced vital capacity.

Discussion

In the present study, we developed and characterized a novel competitive ELISA for the detection of tumstatin (TUM) using a monoclonal antibody detecting a MMP-9 generated neo-epitope fragment of the alpha 3-chain of collagen type IV corresponding to the bioactive molecule tumstatin. The main findings of this study were: i) the assay was technically robust and specific towards the human tumstatin sequence PGLKGKRGDS, ii) the fragment was detectable in human serum and urine and iii) the fragment was significantly elevated in patients with NSCLC compared to IPF patients, COPD patients, and healthy controls, with a high diagnostic accuracy. To our knowledge, this is the first study to develop and validate a specific biomarker of tumstatin and validate it in patients with lung disorders.

TUM was characterized as being a technically robust and sensitive assay, with an IC50 value of 1.6 ng/ml and measurement range from 0.26 ng/ml to 9.92 ng/ml. All technical tests including intra- and intervariation, dilution recovery, interference, and analyte stability gave results within the acceptable range, and the assay specificity test showed that the monoclonal antibody was specific towards the

Table 3. Patient Demographics of Cohort 2

	Healthy Controls (n = 20)	NSCLC (n = 40)	P Value
Age	61.85 (1.95)	61.93 (2.14)	0.593
Male, n (%)	10 (50%)	20 (50%)	1.000
BMI	26.14 (2.67)	25.55 (4.23)	0.533
TUM (ng/ml)	1.26	2.00	0.002

Data are presented as mean (SD) unless otherwise stated. Comparison of age, gender, BMI, and TUM levels was performed using a Mann-Whitney t test. P values below .05 were considered significant.

Table 4. Discriminative Performance of TUM in Healthy Controls and NSCLC

	Cutoff Value (ng/ml)	Sensitivity	Specificity	AUROC (95% CI)	*P*-Value
Cohort 1					
NSCLC vs healthy controls	1.97	100	87.5	0.97 (0.89-1.05)	0.002
NSCLC vs IPF	3.67	87.5	100	0.98 (0.75-1.00)	<0.0001
NSCLC vs COPD	2.37	100	100	1.00 (0.79-1.00)	<0.0001
Cohort 2					
NSCLC vs healthy controls	1.27	100	44	0.73 (0.60-0.84)	0.003
NSCLC stage IV vs healthy controls	1.27	100	60	0.87 (0.73-1.01)	0.001

cleavage site between amino acid 1425 and 1426 located in the alpha 3-chain of collagen type IV.

Our hypothesis was that tumstatin reflected the dysregulated turnover of the BMs [17]. Tumstatin was originally identified by Maeshima et al. [23] and named for its unique property of causing "tumor stasis." In that study tumstatin was shown to inhibit proliferation of vascular endothelial cells and tube formation by *in vitro* and *in vivo* models of angiogenesis and tumor growth [23], having therefore a protective role in cancer development. Decreased serum levels of Col. IV α3 have previously been detected in MMP-9–deficient mice compared to normal mice [13]. This suggested that circulating tumstatin was only present as a consequence of MMP-9–mediated cleavage of COL4α3. Both MMP-9 and COL4α3 need to be upregulated for tumstatin to be generated and detected in human circulation. MMP-9 is known to be upregulated in cancer [24,25], and this could explain why levels of TUM are elevated in serum of patients with NSCLC. Since the fragment detected by TUM can only be found in serum when MMP-9 generates it, our results may suggest that NSCLC patients have a high MMP-9 activity, which increases

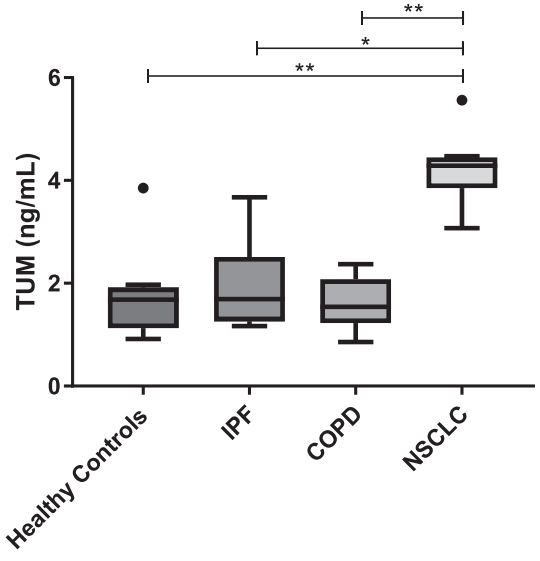

Figure 4. Results from cohort 1. Serum TUM levels was assessed in healthy controls ($n = 8$) and in patients with IPF ($n = 7$), COPD ($n = 8$), and NSCLC ($n = 8$). Data were analyzed using a Kruskal-Wallis test adjusted for Dunn's multiple comparisons test. Data are presented as Tukey boxplots. Significance levels: $*P < 0.05$ and $**P < 0.01$.

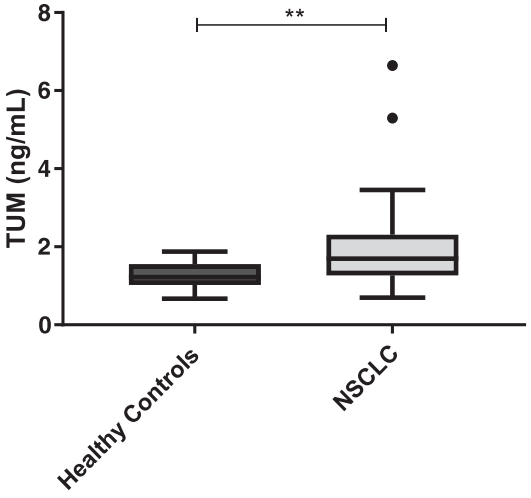

Figure 5. Results from cohort 2. Serum TUM levels was assessed in healthy controls ($n = 20$) and in patients with NSCLC ($n = 40$). Data were analyzed using a Mann-Whitney t test. Data are presented as Tukey boxplots. Significance levels: $**P < 0.01$.

the expression of tumstatin [13,18]. In line with this, MMP-9–generated type I collagen fragments have previously shown potential as biomarkers for NSCLC [26].

In this study, we showed that TUM has a diagnostic potential for NSCLC and is able to separate these patients from patients with lung fibrosis. Based on the high diagnostic accuracy, this could be a biomarker of BM remodeling in lung cancer. High levels of TUM in circulation may indicate disruption of the BM, which can favor cancer invasion [27]. Therefore, TUM may also serve as a marker of tumor activity and severity. As tumstatin appeared to have an antiangiogenic role, TUM may be used as a biomarker to assess the efficacy of antiangiogenic therapies. Antiangiogenic therapies have been extensively studied for the treatment of different cancer types including lung cancer. Despite many of them having been approved for the treatment of cancers, the overall survival benefit has been modest [28]. Biomarkers such as TUM may have the potential to identify the patients most or least likely to benefit from these drugs - a current medical need as there are no validated biomarkers for this purpose [29]. TUM may also be applied to study the intrinsic and acquired resistance mechanisms associated with these antiangiogenic compounds. Thus, based on the present findings and previously described role that many ECM/BM components and specific degradation fragments have in association to the pro- or antiangiogenic activity [17,27,30–38], TUM may have potential as a clinically relevant biomarker for predicting response to treatment. It could furthermore be used to study possible resistance mechanisms to anti-angiogenic compounds.

A limitation of the study lies in the relatively small population sizes and in the cross-sectional design. Moreover, we had limited clinical information on the patients. Nevertheless, we were able to confirm the findings from cohort 1 in cohort 2. Larger longitudinal studies are needed to fully evaluate the potential of TUM as a diagnostic and/or prognostic biomarker for NSCLC.

The assay was evaluated to be technical robust and not interfere with potential substances present in blood. However, whether the age of the samples or hemodialysis interferes with the assay was not analyzed, which is a limitation.

In conclusion, we developed the technically robust competitive ELISA TUM targeting a MMP-9–generated collagen type IV alpha-3 chain fragment known as tumstatin. TUM levels were significantly higher in serum of patients with NSCLC compared to patients with IPF, patients with COPD, and healthy controls. The assay provided high diagnostic accuracy in separating NSCLC patients from those with other lung disorders and from healthy controls. Since tumstatin acts as an inhibitor of tumor growth and has an antiangiogenic role, the marker may be used as a marker of angiogenesis and tumor formation.

Acknowledgements

We would like to thank our laboratory technician Bafren Esmael for help during assay development.

Funding Sources

This work was supported by the Danish Research Fund (Den Danske Forskningsfond).

Conflict of interest

N. Willumsen, S. Sun, T. Manon-Jensen, M. A. Karsdal, and F. Genovese are employed at Nordic Bioscience A/S, which is a company involved in discovery and development of biochemical biomarkers. M. A. Karsdal owns stocks at Nordic Bioscience.

References

[1] Karsdal MA, Nielsen MJ, Sand JM, Henriksen K, Genovese F, and Bay-Jensen A-C, et al (2013). Extracellular matrix remodeling: the common denominator in connective tissue diseases *possibilities for evaluation and current understanding of the matrix as more than a passive architecture, but a key player in tissue failure. Assay Drug Dev Technol* **11**, 70–92 [[Internet] [cited 2017 Jun 23] Available from: http://www.ncbi.nlm.nih.gov/pubmed/23046407].

[2] Colorado PC, Torre A, Kamphaus G, Maeshima Y, Hopfer H, and Takahashi K, et al (2000). Anti-angiogenic cues from vascular basement membrane. *Cancer Res* **60**, 2520–2526.

[3] Pozzi A, Yurchenco PD, and Iozzo RV (2017). The nature and biology of basement membranes. *Matrix Biol* **57-58**, 1–11 [[Internet] [cited 2017 Oct 11] Available from: http://linkinghub.elsevier.com/retrieve/pii/S0945053X16303262].

[4] Glentis A, Gurchenkov V, and Matic Vignjevic D (2014). Assembly, heterogeneity, and breaching of the basement membranes. *Cell Adh Migr* **8**, 236–245 [[Internet] [cited 2017 Oct 17] Available from: http://www.ncbi.nlm.nih.gov/pubmed/24727304].

[5] O'Reilly MS, Boehm T, Shing Y, Fukai N, Vasios G, and Lane WS, et al (1997). Endostatin: an endogenous inhibitor of angiogenesis and tumor growth. *Cell* **88**, 277–285.

[6] Miner JH (2008). Laminins and their roles in mammals. *Microsc Res Tech* **71**, 349–356.

[7] Sannes PL, Wang J. Basement membranes and pulmonary development. Exp Lung Res 1997; 23:101–8. [[Internet]. [cited 2017 Oct 17] Available from http://www.ncbi.nlm.nih.gov/pubmed/9088920]

[8] Randles MJ, Humphries MJ, and Lennon R (2017). Proteomic definitions of basement membrane composition in health and disease. *Matrix Biol* **57-58**, 12–28 [[Internet] [cited 2017 Oct 11] Available from: http://linkinghub.elsevier.com/retrieve/pii/S0945053X16301172].

[9] Gelse K (2003). Collagens—structure, function, and biosynthesis. *Adv Drug Deliv Rev* **55**, 1531–1546 [[Internet] [cited 2014 May 26] Available from: http://linkinghub.elsevier.com/retrieve/pii/S0169409X03001820].

[10] Sand JM, Larsen L, Hogaboam C, Martinez F, Han M, and Røssel Larsen M, et al (2013). MMP mediated degradation of type IV collagen alpha 1 and alpha 3 chains reflects basement membrane remodeling in experimental and clinical fibrosis—validation of two novel biomarker assays. *PLoS One* **8**, e84934 [[Internet] [cited 2014 Sep 18] Available from: http://www.pubmedcentral.nih.gov/articlerender.fcgi?artid=3871599&tool=pmcentrez&rendertype=abstract].

[11] Jarad G, Knutsen RH, Mecham RP, and Miner JH (2016). Albumin contributes to kidney disease progression in Alport syndrome. *Am J Physiol Renal Physiol* **311**, F120–F130 [[Internet] [cited 2017 Oct 17] Available from: http://www.ncbi.nlm.nih.gov/pubmed/27147675].

[12] Foster MH (2017). Basement membranes and autoimmune diseases. *Matrix Biol* **57-58**, 149–168 [[Internet]. Elsevier [cited 2017 Oct 17] Available from: http://www.sciencedirect.com/science/article/pii/S0945053X16301470?via%3Dihub].

[13] Hamano Y, Zeisberg M, Sugimoto H, Lively JC, Maeshima Y, and Yang C, et al (2003). Physiological levels of tumstatin, a fragment of collagen IV a3 chain, are generated by MMP-9 proteolysis and suppress angiogenesis via IVa3 integrin. *Cancer Cell* **3**, 589–601.

[14] Sand JMB, Martinez G, Midjord A-K, Karsdal MA, Leeming DJ, and Lange P (2016). Characterization of serological neo-epitope biomarkers reflecting collagen remodeling in clinically stable chronic obstructive pulmonary disease. *Clin Biochem* **49**, 1144–1151 [[Internet] [cited 2017 Jun 23] Available from: http://www.ncbi.nlm.nih.gov/pubmed/27614218].

[15] Eikesdal HP, Sugimoto H, Birrane G, Maeshima Y, Cooke VG, and Kieran M, et al (2008). Identification of amino acids essential for the antiangiogenic activity of tumstatin and its use in combination antitumor activity. *Proc Natl Acad Sci U S A* **105**, 15040–15045.

[16] Gu Q, Zhang T, Luo J, and Wang F (2006). Expression, purification, and bioactivity of human tumstatin from Escherichia coli. *Protein Expr Purif* **47**, 461–466.

[17] Hamano Y and Kalluri R (2005). Tumstatin, the NC1 domain of α3 chain of type IV collagen, is an endogenous inhibitor of pathological angiogenesis and suppresses tumor growth. *Biochem Biophys Res Commun* **333**, 292–298.

[18] Jiang C-P, Wu B-H, Chen S-P, Fu M-Y, Yang M, and Liu F, et al (2013). High COL4A3 expression correlates with poor prognosis after cisplatin plus gemcitabine chemotherapy in non-small cell lung cancer. *Tumor Biol* **34**, 415–420 [[Internet] [cited 2017 Oct 17] Available from: http://www.ncbi.nlm.nih.gov/pubmed/23108892].

[19] Murphy SL, Xu J, and Kochanek KD (2013). Statistics V. National Vital Statistics Reports Deaths: Final Data for 2010; 2013 61.

[20] Van der Velden J, Harkness LM, Barker DM, Barcham GJ, Ugalde CL, and Koumoundouros E, et al (2016). The effects of tumstatin on vascularity, airway inflammation and lung function in an experimental sheep model of chronic asthma. Sci Rep, 6. Nature Publishing Group; 2016 26309 [[Internet] [cited 2017 Oct 16] Available from: http://www.ncbi.nlm.nih.gov/pubmed/27199164].

[21] Burgess JK, Boustany S, Moir LM, Weckmann M, Lau JY, and Grafton K, et al (2010). Reduction of tumstatin in asthmatic airways contributes to angiogenesis, inflammation, and hyperresponsiveness. Am J Respir Crit Care Med, 181. American Thoracic Society; 2010 106–115 [[Internet] [cited 2017 Oct 17] Available from: http://www.atsjournals.org/doi/abs/10.1164/rccm.200904-0631OC].

[22] Gefter ML, Margulies DH, and Scharff MD (1977). A simple method for polyethylene glycol-promoted hybridization of mouse myeloma cells. *Somatic Cell Genet* **3**, 231–236 [[Internet] Available from: http://www.ncbi.nlm.nih.gov/pubmed/605383].

[23] Maeshima Y, Colorado PC, Torre A, Holthaus KA, Grunkemeyer JA, and Ericksen MB, et al (2000). Distinct antitumor properties of a type IV collagen domain derived from basement membrane. J Biol Chem, 275. American Society for Biochemistry and Molecular Biology; 2000 21340–21348 [[Internet] [cited 2017 Oct 16] Available from: http://www.ncbi.nlm.nih.gov/pubmed/10766752].

[24] Zheng S, Chang Y, Hodges KB, Sun Y, Ma X, and Xue Y, et al (2010). Expression of KISS1 and MMP-9 in non-small cell lung cancer and their relations to metastasis and survival. *Anticancer Res* **30**, 713–718 [[Internet] [cited 2017 Oct 17] Available from: http://www.ncbi.nlm.nih.gov/pubmed/20392988].

[25] El-Badrawy MK, Yousef AM, Shaalan D, and Elsamanoudy AZ (2014). Matrix metalloproteinase-9 expression in lung cancer patients and its relation to serum MMP-9 activity, pathologic type, and prognosis. *J Bronchology Interv Pulmonol* **21**, 327–334 [[Internet]. [cited 2017 Oct 17] Available from: http://www.ncbi.nlm.nih.gov/pubmed/25321452].

[26] Willumsen N, Bager CL, Leeming DJ, Smith V, Christiansen C, and Karsdal MA, et al (2014). Serum biomarkers reflecting specific tumor tissue remodeling processes are valuable diagnostic tools for lung cancer. *Cancer Med* **3**, 1136–1145 [Internet]. [cited 2014 Nov 5] Available from: http://www.ncbi.nlm.nih.gov/pubmed/25044252].

[27] Kalluri R (2003). Basement membranes: structure, assembly and role in tumour angiogenesis. *Nat Rev Cancer* **3**, 422–433.

[28] Jain RK (2013). Normalizing tumor microenvironment to treat cancer: bench to bedside to biomarkers. *J Clin Oncol* **31**, 2205–2218.

[29] Jain RK, Duda DG, Willett CG, Sahani DV, Zhu AX, and Loeffler JS, et al (2009). Biomarkers of response and resistance to antiangiogenic therapy. Nat Rev Clin Oncol, 6. Nature Publishing Group; 2009 327–338.

[30] Sudhakar A, Sugimoto H, Yang C, Lively J, Zeisberg M, and Kalluri R (2003). Human tumstatin and human endostatin exhibit distinct antiangiogenic activities mediated by alpha v beta 3 and alpha 5 beta 1 integrins. *Proc Natl Acad Sci U S A* **100**, 4766–4771.

[31] Dhanabal M, Ramchandran R, Waterman MJ, Lu H, Knebelmann B, and Segal M, et al (1999). Endostatin induces endothelial cell apoptosis. *J Biol Chem* **274**, 11721–11726.

[32] Kim YM, Hwang S, Kim YM, Pyun BJ, Kim TY, and Lee ST, et al (2002). Endostatin blocks vascular endothelial growth factor-mediated signaling via direct interaction with KDR/Flk-1. *J Biol Chem* **277**, 27872–27879.

[33] Maragoudakis ME, Missirlis E, Karakiulakis GD, Sarmonica M, Bastakis M, and Tsopanoglou N (1993). Basement Membrane Biosynthesis as a Target for Developing Inhibitors of Angiogenesis with Anti-Tumor Properties. Kidney Int, 43. Greece: University of Patras Medical School, Department of Pharmacology; 1993 147–150.

[34] Xu J, Rodriguez D, Kim JJ, and Brooks PC (2000). Generation of Monoclonal Antibodies to Cryptic Collagen Sites by Using Subtractive Immunization. Hybridoma, 19. Los Angeles, USA: University of Southern California Keck School of Medicine, Department of Biochemistry and Molecular Biology, Norris Cancer Center; 2000 375–385.

[35] Xu J, Rodriguez D, Petitclerc E, Kim JJ, Hangai M, and Moon YS, et al (2001). Proteolytic exposure of a cryptic site within collagen type IV is required for angiogenesis and tumor growth in vivo. *J. Cell Biol.* **154**, 1069–1079.

[36] Mundel TM and Kalluri R (2007). Type IV collagen-derived angiogenesis inhibitors. Microvasc Res, 74. Boston, MA, USA: Division of Matrix Biology, Department of Medicine, Beth Israel Deaconess Medical Center and Harvard Medical School; 2007 85–89.

[37] O'Reilly MS, Holmgren L, Shing Y, Chen C, Rosenthal RA, and Moses M, et al (1994). Angiostatin: a novel angiogenesis inhibitor that mediates the suppression of metastases by a Lewis lung carcinoma. *Cell* **79**, 315–328.

[38] Chang JH, Javier JA, Chang GY, Oliveira HB, and Azar DT (2005). Functional characterization of neostatins, the MMP-derived, enzymatic cleavage products of type XVIII collagen. *Febs Lett* **579**, 3601–3606.